The following Communications have been judged by at least two referees to be “very important papers” and will be published online at www.angewandte.org soon:

*S. T. Scroggins, Y. Chi, J. M. J. Fréchet**
Polarity-Directed One-Pot Asymmetric Cascade Reactions Mediated by Two Catalysts in an Aqueous Buffer

*S. Saito, Ko Furukawa, A. Osuka**
T-Shaped Three-Coordinate Copper(II) Heptaphyrin Complexes with a Supplementary Copper(II)–Arene Interaction

*A. B. Chaplin, A. S. Weller**
B–H Activation at a Rhodium(I) Center: A Missing Link in the Transition-Metal-Catalyzed Dehydrocoupling of Amine–Boranes

*G. de Ruiter, E. Tartakovsky, N. Oded, M. E. van der Boom**
Sequential Logic Operations with Surface-Confined Polypyridyl Complexes Having Molecular Random Access Memory Features

*W. Li, P. H. C. Camargo, L. Au, Q. Zhang, M. Rycenga, Y. Xia**
Etching and Dimerization: A Simple and Versatile Route to Dimers of Silver Nanospheres with a Range of Sizes

*I. U. Khan, D. Zwanziger, I. Böhme, M. Javed, H. Naseer, S. W. Hyder, A. G. Beck-Sickinger**
Breast Cancer Diagnosis by Neuropeptide Y Analogues: From Synthesis to Clinical Application

*K. Fesko, M. Uhl, J. Steinreiber, K. Gruber, H. Griengl**
Biocatalytic Access to α,α-Dialkyl-α-Amino Acids by a Mechanism-Based Approach

Y.-S. Li, F.-Y. Liang, H. Bux, A. Feldhoff, W.-S. Yang, J. Caro**
Metal–Organic Framework Molecular Sieve Membrane: Supported ZIF-7 Layer with High Hydrogen Selectivity by Microwave-Assisted Seeded Growth

S. Yamago, Y. Watanabe, T. Iwamoto*
Synthesis of [8]Cycloparaphenylene from a Square-Shaped Tetranuclear Platinum Complex $[\{Pt(cod)(4,4'\text{-biphenyl})\}_4]$

S. M. Lang, T. M. Bernhardt, R. N. Barnett, U. Landman**
Methane Activation and Catalytic Ethylene Formation on Free Au_2^+

Author Profile

“The biggest challenge facing scientists is the highly effective use of solar energy. If I could be anyone for a day, I would be Michael Jordan …”
This and more about Masaki Shimizu can be found on page 9778.

News

S.V. Ley

E. Nakamura

S. W. Hell

Books

Highlights

Catalyst Design

T. Bligaard* ________ **9782 – 9784**

Linear Energy Relations and the Computational Design of Selective Hydrogenation/Dehydrogenation Catalysts

Mind over matter: Electronic structure calculations have been used to establish linear energy relations for chemical reactions on solid surfaces which aid in the design of new catalytic materials. Newly discovered accurate linear relations for the hydrogenation of organic molecules on transition metals suggest that the computational design of selective hydrogenation catalysts for complex reactions may soon be feasible.

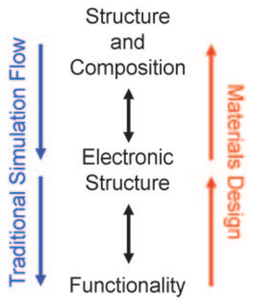

Catalysis with Light

K. Zeitler* ________ **9785 – 9789**

Photoredox Catalysis with Visible Light

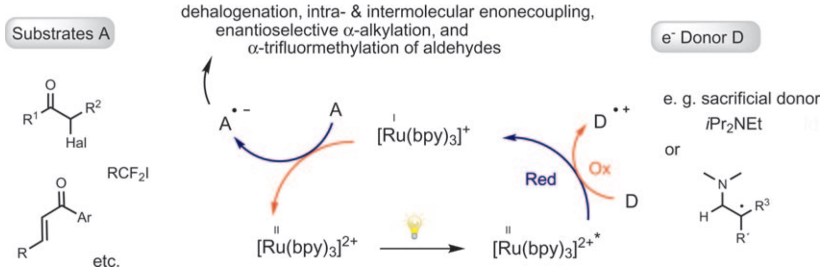

On the sunny side: Recent examples of visible-light-promoted photoredox catalysis in the presence of $[Ru(bpy)_3]^{2+}$ as an efficient photocatalyst have set new standards for conducting challenging reactions under mild and environmentally benign conditions.

Reviews

C–H Functionalization

L. Ackermann,* R. Vicente,
A. R. Kapdi ________ **9792 – 9826**

Transition-Metal-Catalyzed Direct Arylation of (Hetero)Arenes by C–H Bond Cleavage

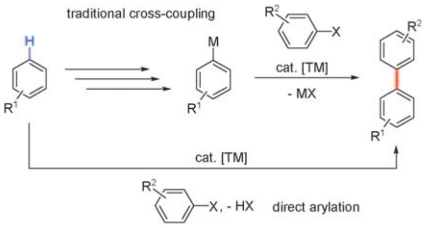

Cutting across: Direct arylations are increasingly viable alternatives to conventional cross-coupling reactions with stoichiometric amounts of organometallic reagents (see Scheme). This Review summarizes recent progress in the rapidly evolving research area of transition-metal-catalyzed C–H bond-cleavage reactions for (hetero)aryl syntheses.

For the USA and Canada: ANGEWANDTE CHEMIE International Edition (ISSN 1433-7851) is published weekly by Wiley-VCH, PO Box 191161, 69451 Weinheim, Germany. Air freight and mailing in the USA by Publications Expediting Inc., 200 Meacham Ave., Elmont, NY 11003. Periodicals postage paid at Jamaica, NY 11431. US POSTMASTER: send address changes to *Angewandte Chemie*, Wiley-VCH, 111 River Street, Hoboken, NJ 07030. Annual subscription price for institutions: US$ 9442/8583 (valid for print and electronic / print or electronic delivery); for individuals who are personal members of a national chemical society prices are available on request. Postage and handling charges included. All prices are subject to local VAT/sales tax.

Communications

Chemical Shifts

S. N. Steinmann, D. F. Jana, J. I.-C. Wu,
P. v. R. Schleyer, Y. Mo,
C. Corminboeuf* ________ **9828 – 9833**

Direct Assessment of Electron Delocalization Using NMR Chemical Shifts

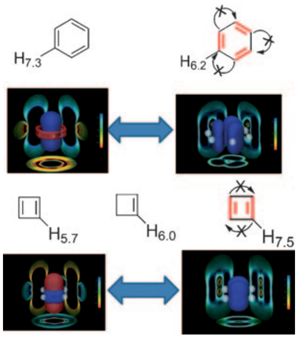

Probe it: The new BLW-IGLO approach evaluates the magnetic responses of molecules in which conjugative interactions are “disabled” (see picture, red bonds). The NMR spectroscopy parameters of the localized structures provide ideal non-aromatic olefinic hydrogen $\delta(^1H)$ references for the fully conjugated systems.

Asymmetric Catalysis

Y. Wang, R.-G. Han, Y.-L. Zhao, S. Yang,
P.-F. Xu,* D. J. Dixon* ____ **9834 – 9838**

Asymmetric Organocatalytic Relay Cascades: Catalyst-Controlled Stereoisomer Selection in the Synthesis of Functionalized Cyclohexanes

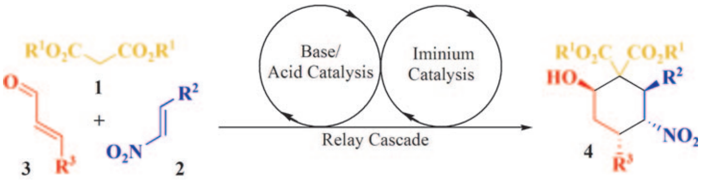

Passing the baton: A relay cascade process provides cyclohexanes in a direct, efficient, and stereoselective manner. The triple-cascade reaction is efficient, affords high selectivities, and has a broad scope, and different diastereomers are readily accessible by judicious choice of organocatalysts.

CO_2 Reduction

A. E. Ashley,* A. L. Thompson,
D. O’Hare* ____________ **9839 – 9843**

Non-Metal-Mediated Homogeneous Hydrogenation of CO_2 to CH_3OH

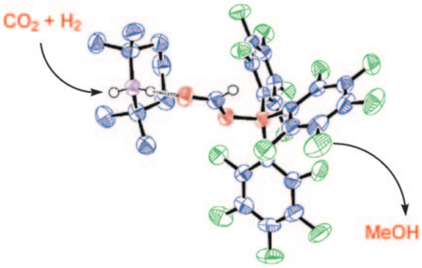

Turning a problem to advantage: CO_2, a contributor to global warming, was converted into the valuable resource CH_3OH by adding it to 2,2,6,6-tetramethylpiperidine and $B(C_6F_5)_3$ in toluene under H_2 (1–2 atm), heating the mixture at 160 °C, and vacuum distillation. CH_3OH was formed via the complex shown (C blue, N purple, O red, B orange, F green) as the sole C_1 product.

Main-Group Chemistry

J. I. Bates, P. Kennepohl,
D. P. Gates* ___________ **9844 – 9847**

Abnormal Reactivity of an N-Heterocyclic Carbene (NHC) with a Phosphaalkene: A Route to a 4-Phosphino-Substituted NHC

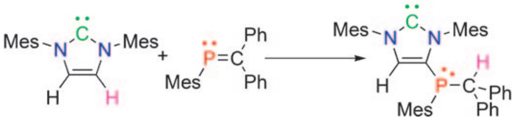

A naughty NHC: A stable N-heterocyclic carbene (NHC) reacts with a phosphaalkene not at the expected 2-position, but through the 4-position, which leads to an unprecedented 4-phosphino-substituted NHC that functions as a novel bifunctional ligand for gold(I). The mechanism of this reaction has been investigated using density functional calculations.

Frontiers of Chemistry:
From Molecules to Systems
A One-Day Symposium

Celebrating 10 Years of

On 21st May 2010 in Paris
at the Maison de la Chimie
(near the Eiffel Tower and Les Invalides)

Speakers


Gerhard Ertl
Nobel Prize 2007


Jean-Marie Lehn
Nobel Prize 1987


Roger Y. Tsien
Nobel Prize 2008


Ada Yonath
Nobel Prize 2009


Luisa De Cola


Alan R. Fersht


Marc Fontecave


Michael Grätzel


Michel Orrit


Nicolas Winssinger

Scientific committee

E. Amouyal, M. Che,
F. C. De Schryver,
A. R. Fersht, P. Gölitz,
J. T. Hynes, J.-M. Lehn

Posters

will be displayed also online from 1st April.

www.chembiophyschem.org

Topics

catalysis, biochemical imaging, chemical biology, bionanotechnology, proteomics, spectroscopy, solar cells

ChemPubSoc Europe

SCF
Société Chimique de France

WILEY-VCH

Organocatalysis

H. Uehara, C. F. Barbas III* **9848 – 9852**

anti-Selective Asymmetric Michael Reactions of Aldehydes and Nitroolefins Catalyzed by a Primary Amine/Thiourea

It's finally here: Highly *anti*-selective Michael reactions of a functionalized aldehyde with nitroolefins have been realized using a primary amine/thiourea catalyst (see scheme; TBS = *tert*-butyldimethylsilyl). The reaction relies on a conformational strategy based on directing the formation of a *Z*-configured enamine intermediate.

Cyclobutadiene Hopping

T. A. Albright, P. I. Dosa,
T. N. Grossmann, V. N. Khrustalev,
O. A. Oloba, R. Padilla, R. Paubelle,
A. Stanger, T. V. Timofeeva,
K. P. C. Vollhardt* **9853 – 9857**

Photo–Thermal Haptotropism in Cyclopentadienylcobalt Complexes of Linear Phenylenes: Intercyclobutadiene Metal Migration

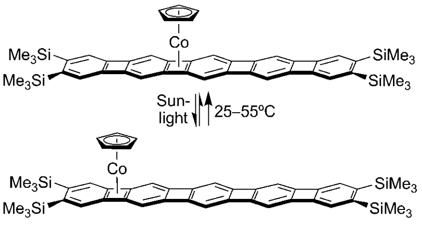

The CpCo-shuffle: {CpCo} complexes of linear [3]- and [5]phenylene undergo a light-induced haptotropic migration from a more strongly bound cyclobutadiene moiety to a less strongly bound (see scheme). The shift is thermally reversible and proceeds along the periphery of the intervening arene rings. As such, the systems constitute photo–thermal storage systems, as well the first examples of cyclobutadiene-to-cyclobutadiene haptotropism.

Fluorinated Alkenes

W. Zhang, W. Huang, J. Hu* **9858 – 9861**

Highly Stereoselective Synthesis of Monofluoroalkenes from α-Fluorosulfoximines and Nitrones

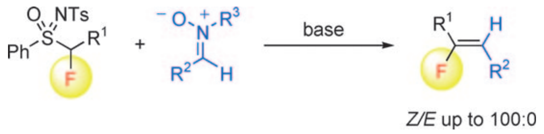

A fine fusion: α-fluorosulfoximines readily react with simple nitrones to give monofluoroalkenes with excellent *E*/*Z* stereocontrol (see scheme). This novel fluoroolefination method shows promising applications in medicinal chemistry as monofluoroalkenes are potential mimetics for peptide units as protein inhibitors.

Immunoassay

H. Nie, S. Liu, R. Yu,
J. Jiang* **9862 – 9866**

Phospholipid-Coated Carbon Nanotubes as Sensitive Electrochemical Labels with Controlled-Assembly-Mediated Signal Transduction for Magnetic Separation Immunoassay

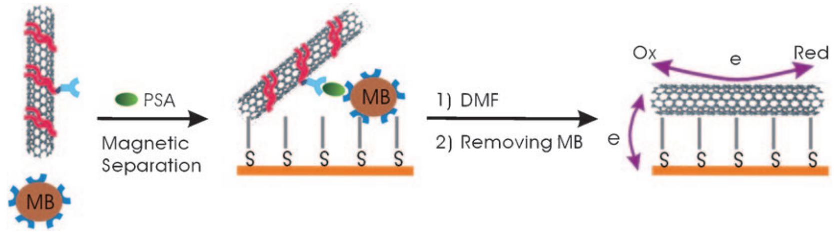

A coat to note: An electrochemical immunoassay strategy is developed using phospholipid-coated multiwalled carbon nanotubes (MWNTs) as the electrochemical labels (see scheme; PSA = antigen protein; MB = magnetic bead). This strategy affords great sensitivity and specificity in signal transduction.

Contents

Drug Delivery

J. T. F. Keurentjes,* M. F. Kemmere,
H. Bruinewoud, M. A. M. E. Vertommen,
S. A. Rovers, R. Hoogenboom,
L. F. S. Stemkens, F. L. A. M. A. Péters,
N. J. C. Tielen, D. T. A. van Asseldonk,
A. F. Gabriel, E. A. Joosten,
M. A. E. Marcus ________ **9867 – 9870**

Externally Triggered Glass Transition Switch for Localized On-Demand Drug Delivery

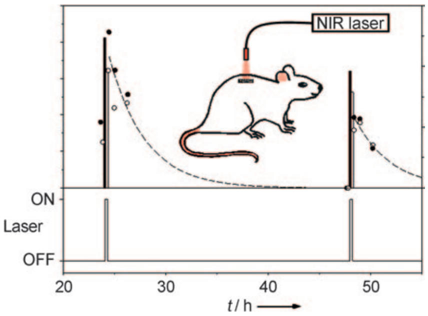

I want a new drug dose: External on-demand laser triggering is used in a drug-delivery concept, with on/off ratios in excess of 1000/1. The switching mechanism involves the glass transition of hydrophobic polymers with a large change in diffusivity. Formation of a glassy surface layer of the implant in the off state plays a key role, resulting in negligible off-release. (Picture: data points indicate ibuprofen concentration).

Polymerization

C. De Rosa,* F. Auriemma,
L. Resconi ________ **9871 – 9874**

Metalloorganic Polymerization Catalysis as a Tool To Probe Crystallization Properties of Polymers: The Case of Isotactic Poly(1-butene)

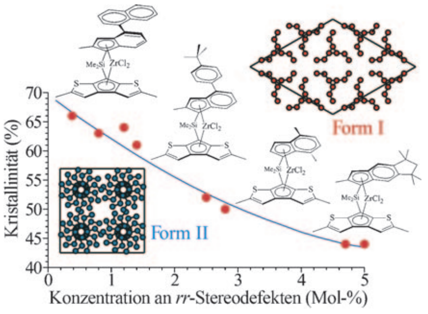

Age shall not weary them: Stereodefective isotactic polybutene samples, synthesized with single-center metallocene catalysts, crystallize from the melt into the stable form I (see picture) and do not undergo phase transformation upon aging at room temperature. Hence, the corresponding physical and mechanical properties of molded objects are not altered by aging.

Asymmetric Catalysis

K. Komeyama,* N. Saigo, M. Miyagi,
K. Takaki* ________ **9875 – 9878**

Intramolecular Alkynylcyclopropanation of Olefins Catalyzed by $Bi(OTf)_3$: Stereoselective Synthesis of 1-Alkynyl-3-azabicyclo[3.1.0]hexanes

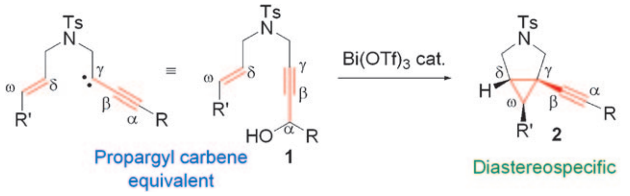

The postman always rings twice: 1-Alkynyl-3-azabicyclo[3.1.0]hexanes **2** were obtained in good to excellent yields from the stereoselective $Bi(OTf)_3$-catalyzed dehydrative alkynylcyclopropanation of azaenynols **1**, in which the propargyl alcohol motif of **1** acted as a propargyl carbene synthetic equivalent.

Click Chemistry

V. Hong, S. I. Presolski, C. Ma,
M. G. Finn* ________ **9879 – 9883**

Analysis and Optimization of Copper-Catalyzed Azide–Alkyne Cycloaddition for Bioconjugation

How to click with biomolecules: Copper-catalyzed azide–alkyne cycloaddition has been optimized for use with biological molecules. The key development is the addition of two reagents that allow ascorbate to be used as reducing agent whilst eliminating problems caused by copper ascorbate side reactions. The result is a robust, rapid, and convenient procedure for the modification of proteins, DNA, RNA, and other biomolecules (see scheme).

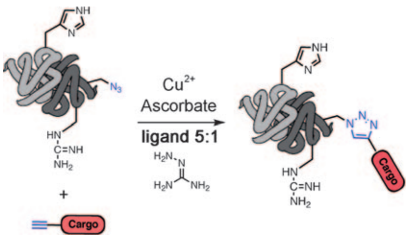

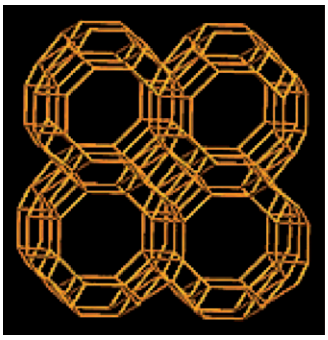

The RTH-type zeolite (see picture) has an attractive pore structure, but its compositional variation is limited. Now, metallosilicates with the RTH-topology can be synthesized by two routes, one of which does not use structure-directing agents. Thus prepared Al-containing RTH-type zeolites exhibited a remarkable catalytic performance for the methanol-to-olefins reaction, producing propene with high selectivity.

Zeolites

T. Yokoi,* M. Yoshioka, H. Imai,
T. Tatsumi* ———— **9884 – 9887**

Diversification of RTH-Type Zeolite and Its Catalytic Application

---

Urea as a nitrogen source: The supported ruthenium hydroxide, Ru(OH)$_x$/TiO$_2$, acts as an efficient heterogeneous catalyst for the title reaction. The retrieved catalyst after the reaction could be reused without a significant loss of its catalytic performance.

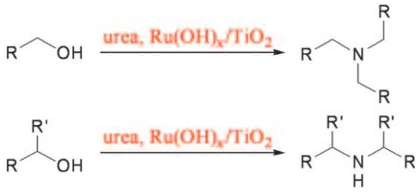

Amine Synthesis

J. L. He, J. W. Kim, K. Yamaguchi,
N. Mizuno* ———— **9888 – 9891**

Efficient Catalytic Synthesis of Tertiary and Secondary Amines from Alcohols and Urea

---

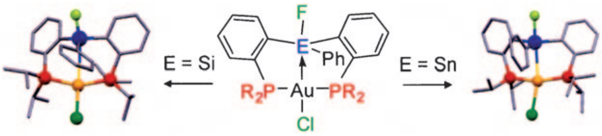

Gold gets a grip: Spectroscopic, structural, and computational results provide evidence for unprecedented Au→Si and Au→Sn interactions in gold(I) complexes derived from diphosphino-substituted silane and stannane ligands (see scheme).

σ-Acceptor Ligands

P. Gualco, T.-P. Lin, M. Sircoglou,
M. Mercy, S. Ladeira, G. Bouhadir,
L. M. Pérez, A. Amgoune, L. Maron,*
F. P. Gabbaï,*
D. Bourissou* ———— **9892 – 9895**

Gold–Silane and Gold–Stannane Complexes: Saturated Molecules as σ-Acceptor Ligands

---

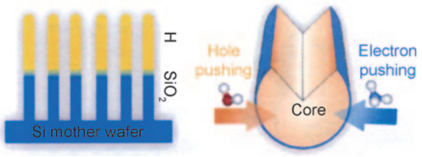

Staying on top: Altering the surface of silicon nanowires (SiNWs) by terminating the surface with different species and/or introducing surface adsorbates can change the electrical properties of the SiNWs. Such easy, nondestructive conductivity modification would expand possible applications of SiNWs.

Passivation Doping

C. S. Guo, L. B. Luo, G. D. Yuan,
X. B. Yang, R. Q. Zhang,* W. J. Zhang,
S. T. Lee* ———— **9896 – 9900**

Surface Passivation and Transfer Doping of Silicon Nanowires

Contents

Coordination Polymers

K. E. deKrafft, Z. Xie, G. Cao, S. Tran, L. Ma, O. Z. Zhou, W. Lin* **9901 – 9904**

Iodinated Nanoscale Coordination Polymers as Potential Contrast Agents for Computed Tomography

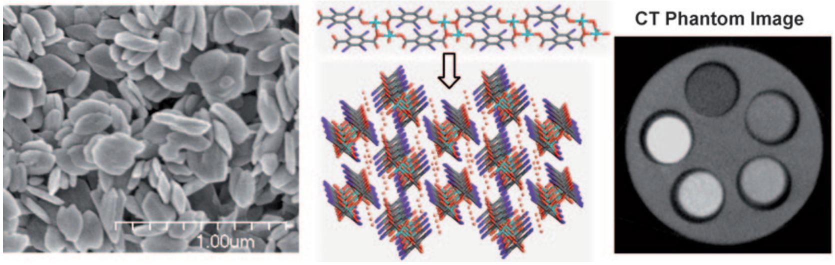

Nanoscale coordination polymers (NCPs), prepared with metal ions and an iodinated ligand, were synthesized using reverse-phase microemulsion techniques and rapid precipitation procedures. The NCPs carry high payloads of iodine (ca. 63 wt %) and have potential applications as a new class of contrast agents for computed tomography (CT), as demonstrated by phantom studies (see figure).

Metal–Organic Frameworks

L. Ma, A. Jin, Z. Xie, W. Lin* **9905 – 9908**

Freeze Drying Significantly Increases Permanent Porosity and Hydrogen Uptake in 4,4-Connected Metal–Organic Frameworks

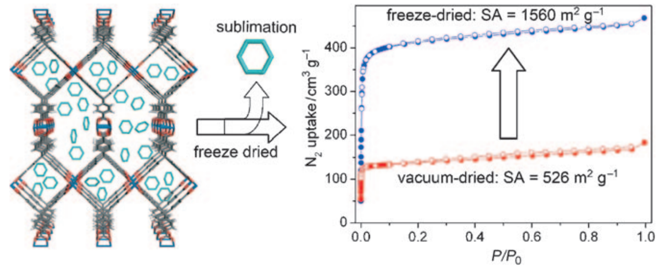

Freeze the flood: After replacing high boiling-point solvents inside the channels of a metal–organic framework (MOF), benzene is frozen and then removed under vacuum by sublimation. Bypassing the liquid phase eliminates the detrimental effects of surface tension that induce mesopore collapse in MOFs, thereby enhancing their permanent porosity and hydrogen-uptake capacity (see scheme).

Nanostructures

Y. Chen, K. Li, W. Lu,* S. S.-Y. Chui, C.-W. Ma, C.-M. Che* **9909 – 9913**

Photoresponsive Supramolecular Organometallic Nanosheets Induced by $Pt^{II}\cdots Pt^{II}$ and C–H$\cdots\pi$ Interactions

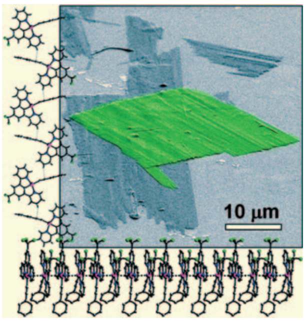

It's a flat world: Charge-neutral pincer-type cyclometalated platinum(II) aryl acetylides can be assembled into quasi-two-dimensional nanosheets through bilateral intermolecular noncovalent interactions (see picture). These nanosheets can be further self-organized into layered materials on a flat substrate and exhibit NIR phosphorescence and light-modulated conductivity.

Drug Delivery

Y.-L. Li, L. Zhu, Z. Liu, R. Cheng, F. Meng,* J.-H. Cui, S.-J. Ji, Z. Zhong* **9914 – 9918**

Reversibly Stabilized Multifunctional Dextran Nanoparticles Efficiently Deliver Doxorubicin into the Nuclei of Cancer Cells

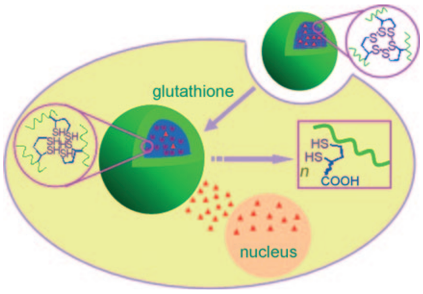

Getting in there: Efficient intracellular delivery of anticancer drugs is achieved by using reversibly cross-linked dextran nanoparticles, which are rapidly destabilized under reductive environments that mimic those of the intracellular compartments. These nanoparticles show high drug loading efficiency and reduction-triggered release of doxorubicin in vitro as well as inside tumor cells, particularly to the cell nucleus (see scheme).

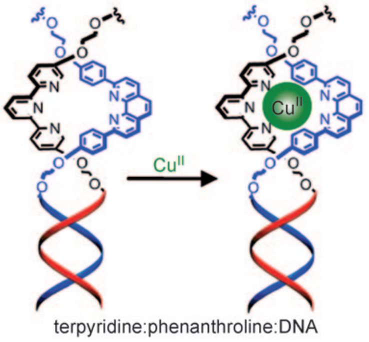

Each to his own: DNA templates the formation of bis(terpyridine), bis(phenanthroline), and terpyridine:phenanthroline ligand environments, which strongly bind Fe^{II}, Cu^{I}, and Cu^{II} (see picture), respectively, to generate highly stable metal–DNA complexes. When a metal is placed in the "incorrect" environment, it can spontaneously adjust its redox state, be displaced by another metal, or reorganize the coordination site to create a more favored complex.

Metal–DNA Structures

H. Yang, A. Z. Rys, C. K. McLaughlin, H. F. Sleiman* ____ **9919–9923**

Templated Ligand Environments for the Selective Incorporation of Different Metals into DNA

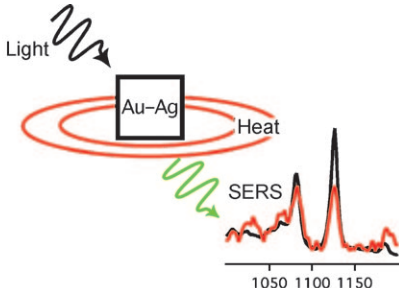

A spectral thermometer: The conformation of molecules on a metallic nanoparticle's surface is sensitive to temperature variations and can be easily monitored in situ by surface-enhanced Raman scattering (SERS). Excitation of the metallic nanoparticle for SERS can concurrently induce a photothermal effect whereby the light absorbed by the nanoparticle is released as heat. From the SERS spectra, the changes in temperature during the photothermal effect can be derived (see picture).

Photothermal Effect

M. Rycenga, Z. Wang, E. Gordon, C. M. Cobley, A. G. Schwartz, C. S. Lo, Y. Xia* ____ **9924–9927**

Probing the Photothermal Effect of Gold-Based Nanocages with Surface-Enhanced Raman Scattering (SERS)

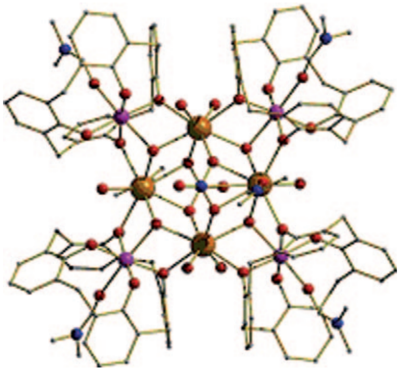

Chilling out: The first 3d/4f cluster based on calix[4]arenes (see picture; purple Mn, brown Gd, red O, blue N) has a high magnetic isotropy and a large number of molecular spin states that are populated even at low temperatures, whereas its ferromagnetic limit is approached only at high applied fields. These results enable the complex to be an excellent magnetic refrigerant for low-temperature applications.

Magnetism

G. Karotsis, M. Evangelisti, S. J. Dalgarno,* E. K. Brechin* ____ **9928–9931**

A Calix[4]arene 3d/4f Magnetic Cooler

Hot and cold: The high degree of localization in SERS hot spots is demonstrated directly by a selective deposition of Raman analytes inside and outside the field-enhanced regions in a plasmonic cavity (see picture). The localization is demonstrated by measurements of both the absolute SERS intensities and the kinetics for photoinduced degradation at different positions.

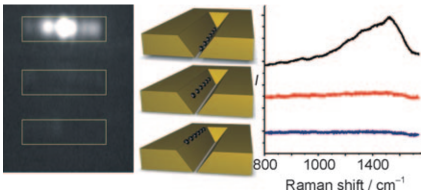

Localized SERS

C. Chen,* J. A. Hutchison, F. Clemente, R. Kox, H. Uji-I, J. Hofkens, L. Lagae, G. Maes, G. Borghs, P. Van Dorpe* ____ **9932–9935**

Direct Evidence of High Spatial Localization of Hot Spots in Surface-Enhanced Raman Scattering

Contents

Conjugated Oligomers

J.-S. Yang,* J.-L. Yan, C.-K. Lin, C.-Y. Chen, Z.-Y. Xie, C.-H. Chen ——— **9936 – 9939**

Pentiptycene-Derived Oligo(*p*-phenyleneethynylene)s: Conformational Control, Chain-Length Effects, Localization of Excitation, and Intrachain Resonance Energy Transfer

Do the twist: The preference of large pentiptycene–pentiptycene dihedral angles and the restricted torsional relaxation for pentiptycene-derived oligo(*p*-phenyleneethynylene)s in a 2-methyltetrahydrofuran glass at 80 K result in a localized excited state. These results demonstrate not only the concept of torsion-induced localization of excitation but also the efficient intrachain energy hopping processes in conjugated polymers.

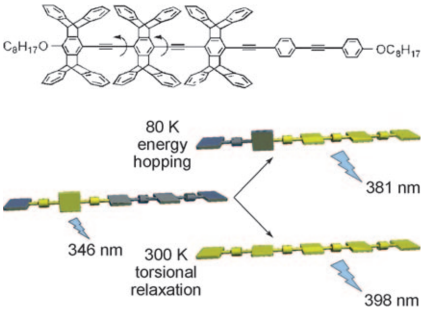

VIP

Total Synthesis (1)

G. W. O'Neil, J. Ceccon, S. Benson, M.-P. Collin, B. Fasching, A. Fürstner* ——— **9940 – 9945**

Total Synthesis of Spirastrellolide F Methyl Ester—Part 1: Strategic Considerations and Revised Approach to the Southern Hemisphere

In readiness for closure: To ensure optimal convergence in the projected total synthesis of spirastrellolide F, the building block representing the southern hemisphere was prepared with a free carboxylic acid and an enol triflate (Tf) terminus (see picture). This unusual pattern allows the 38-membered macrocyclic core of this potent antimitotic agent to be constructed, while keeping late-stage protecting-group manipulations to a minimum.

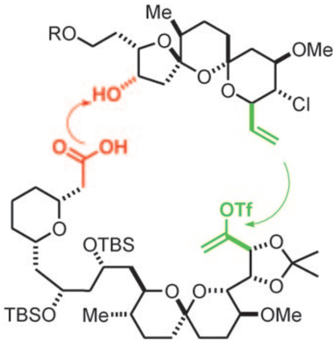

VIP

Total Synthesis (2)

S. Benson, M.-P. Collin, G. W. O'Neil, J. Ceccon, B. Fasching, M. D. B. Fenster, C. Godbout, K. Radkowski, R. Goddard, A. Fürstner* ——— **9946 – 9950**

Total Synthesis of Spirastrellolide F Methyl Ester—Part 2: Macrocyclization and Completion of the Synthesis

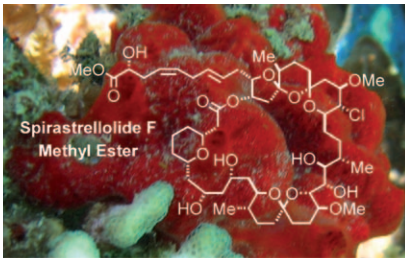

Marvel of the sea: A concise and highly convergent total synthesis of the methyl ester of the marine macrolide spirastrellolide F (see picture), which has exquisite antimitotic properties, is reported. In this approach, the northern and the southern hemispheres of this intricate target are stitched together in only two consecutive steps (Suzuki coupling, Yamaguchi lactonization) without any interim protecting-group manipulations.

Conductive Organic Crystals

L. Jiménez-García, A. Kaltbeitzel, W. Pisula, J. S. Gutmann, M. Klapper,* K. Müllen* ——— **9951 – 9953**

Phosphonated Hexaphenylbenzene: A Crystalline Proton Conductor

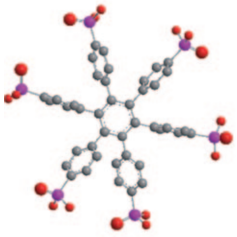

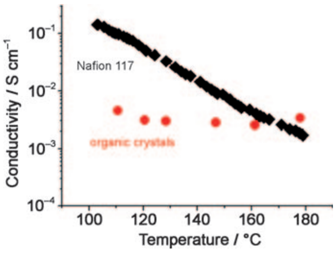

Well stacked: Organic crystals of small molecules constitute an alternative to common polymeric electrolytes (Nafion 117) and inorganic crystals that are employed as proton exchange membranes in fuel cell systems. A phosphonic acid containing hexaphenylbenzene forms a columnar supramolecular array and exhibits a high and constant intrinsic conductivity of 3.2×10^{-3} S cm^{-1} from 120 to 180 °C under 1 bar H_2O atmosphere (see picture).

MOF for more gas storage: A new mesoporous metal–organic framework (MOF) with extremely high adsorption capacities for methane, H_2, and *n*-butane is prepared from the reaction of H_3(btb), H_2(2,6-ndc), and zinc nitrate (btb = benzene-1,3,5-tribenzoate; 2,6ndc = 2,6-naphthalenedicarboxylate). The main structural motif is a dodecahedron formed from 12 Zn_4O^{6+} clusters, four 2,6-ndc, and eight btb linkers (see picture; green: Zn_4O^{6+}, gray: C, red: O; the red sphere illustrates the pore volume).

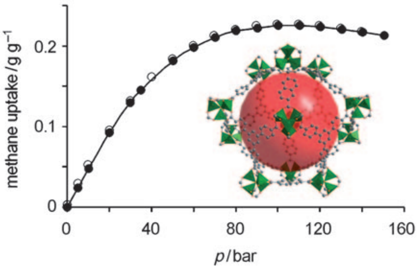

Porous Materials

N. Klein, I. Senkovska, K. Gedrich,
U. Stoeck, A. Henschel, U. Mueller,
S. Kaskel* ———— **9954 – 9957**

A Mesoporous Metal–Organic Framework

Larger lithium clusters than tetrahedral and octahedral Li_n aggregates can be prepared as cage structures with a central anion. The central chlorine atom (green) serves as a template for the formation of a Li_{12} icosahedral cage (orange), which is stabilized by 1,4-butanediide "clamps" (C gray).

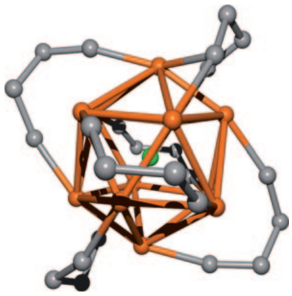

Organolithium Compounds

R. Fischer, H. Görls,
M. Westerhausen* ———— **9958 – 9961**

A Dilithium 1,4-Butanediide with a Chlorine-Centered Li_{12} Icosahedral Structure

---

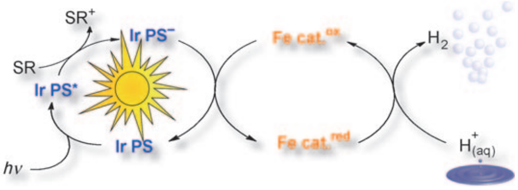

Let your light shine: A novel state-of-the-art system for light-driven proton reduction with iron catalysts was developed (see scheme; SR = sacrificial reagent). It consists of simple iron carbonyl complexes such as $[Fe_3(CO)_{12}]$, triethylamine as sacrificial reagent (electron donor), and $[Ir(bpy)(ppy)_2]PF_6$ as photosensitizer (PS). High turnover numbers of more than 3000 for the sensitizer and 400 for the iron catalyst are obtained.

Hydrogen Generation

F. Gärtner, B. Sundararaju, A.-E. Surkus,
A. Boddien, B. Loges, H. Junge,
P. H. Dixneuf, M. Beller* —— **9962 – 9965**

Light-Driven Hydrogen Generation: Efficient Iron-Based Water Reduction Catalysts

---

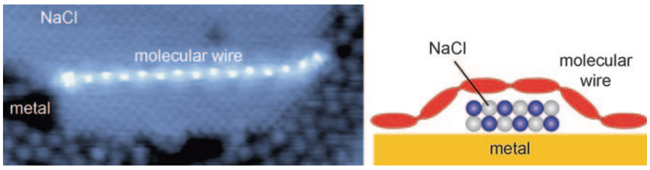

Totally wired: A particular molecular adsorption geometry can be prepared by adsorbing single conjugated polyfluorene chains partially on a clean Au(111) surface and partially on a thin crystalline NaCl film, thus connecting metallic and insulating surface areas. This configuration allows the electronic characterization of one and the same molecular wire as a function of its atomic-scale environment in a planar configuration.

Molecular Wires

C. Bombis, F. Ample, L. Lafferentz, H. Yu,
S. Hecht, C. Joachim,
L. Grill* ———— **9966 – 9970**

Single Molecular Wires Connecting Metallic and Insulating Surface Areas

Annulenes

G. Bucher,* S. Grimme,* R. Huenerbein,
A. A. Auer,* E. Mucke, F. Köhler,
J. Siegwarth, R. Herges* ____ **9971 – 9974**

Is the [9]Annulene Cation a Möbius Annulene?

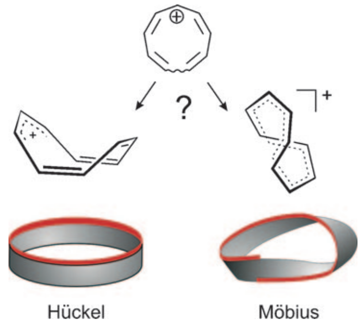

Does it do the twist? High-level theoretical calculations show that the [9]annulene cation exists in two isomers: a twisted $4n$ electron Möbius aromatic compound, and a non-twisted boat-like Hückel conformation (see scheme). The latter form was detected by laser flash photolysis experiments; an example of a stable, charged, or uncharged parent Möbius annulene is still elusive.

Organocatalysis

S. Müller, B. List* ________ **9975 – 9978**

A Catalytic Asymmetric 6π Electrocyclization: Enantioselective Synthesis of 2-Pyrazolines

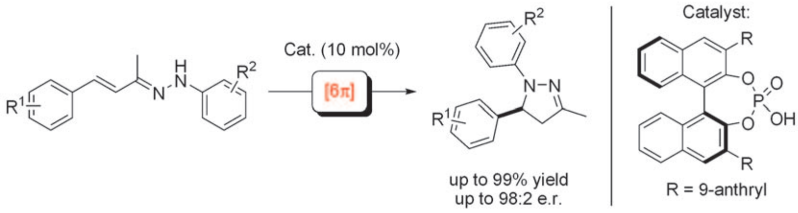

A closer look at α,β-unsaturated hydrazonium ions reveals that they are isoelectronic to the pentadienyl anion, making them suitable substrates to undergo 6π electrocyclizations. The enantioselective catalysis of this transformation is achieved for the first time by asymmetric Brønsted acid catalysis.

Organocatalysis

E. E. Maciver, S. Thompson,
M. D. Smith* ____________ **9979 – 9982**

Catalytic Asymmetric 6π Electrocyclization: Enantioselective Synthesis of Functionalized Indolines

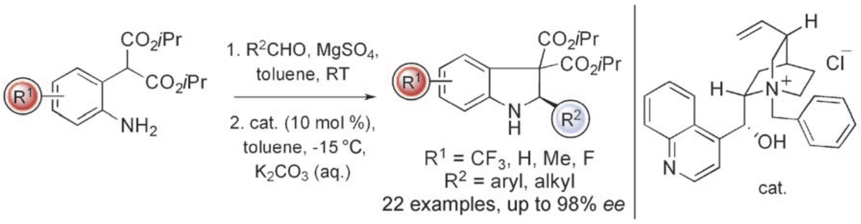

How to close a ring: An approach to catalytic asymmetric 6π electrocyclization leads to a highly enantioselective process that was used in the synthesis of chiral indolines (see scheme). Treatment of *N*-aryl imines under phase transfer conditions in the presence of *N*-benzyl cinchonidinium chloride generates a delocalized 2-aza-pentadienyl anion system that cyclizes in up to 99 % yield and 98 % *ee*.

Supporting information is available on www.angewandte.org (see article for access details).

A video clip is available as Supporting Information on www.angewandte.org (see article for access details).

Service

Corrigendum

The authors of this Communication have recognized an error in Scheme 1. The correct Scheme 1 is shown here.

The text which refers to this Scheme (page 4597, left column) is also incorrect. It should read: "This observation suggests two alternative mechanisms for chain release coupled to isochromanone formation, to yield the putative intermediate deshydroxyajudazol B (**3**) (Scheme 1): TE-catalyzed attack of the C9 hydroxy group of the chain onto the acyl ester bond to give the free ten-membered ring lactone, followed by C2–C7 aldol addition and ring I aromatization; or b) aldol addition/aromatization to form ring I while the intermediate remains tethered to the TE, followed by TE-catalyzed lactonization and chain release to yield ring II."

The authors would like to point out that this error does not affect the interpretation of data in the manuscript.

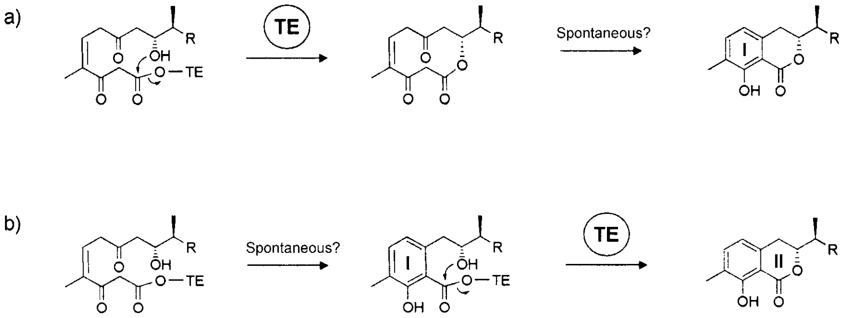

Scheme 1. Proposed mechanism for formation of the isochromanone ring system and chain release. a) The TE catalyzes lactone ring formation, which is followed by aldol addition and aromatization of ring I. b) Aldol addition and aromatization occur to generate ring I, followed by TE-catalyzed lactonization and chain release to afford ring II.

Production of the Antifungal Isochromanone Ajudazols A and B in *Chondromyces crocatus* Cm c5: Biosynthetic Machinery and Cytochrome P450 Modifications

K. Buntin, S. Rachid, M. Scharfe,
H. Blöcker, K. J. Weissman,
R. Müller* ______________ **4595–4599**

Angew. Chem. Int. Ed. **2008**, *47*

DOI 10.1002/anie.200705569

Corrigendum

In the Communication on page 8141 (as well as in the inside cover text on page 7942 and in the table of contents on page 7956) in issue 43, the name of one author was misspelled. The correct name is W. Klopper. The editorial office apologizes for this mistake.

Snapshots of the Al–Al σ-Bond Formation Starting from $\{AlR_2\}$ Units: Experimental and Computational Observations

P. Henke, T. Pankewitz, W. Klopper,*
F. Breher, H. Schnöckel* ___ **8141–8145**

Angew. Chem. Int. Ed. **2009**, *48*

DOI 10.1002/anie.200901754